Molecular Biology of the Cell
Vol. 13, 3431–3440, October 2002

Radiation-induced Activation of Nuclear Factor-κB Involves Selective Degradation of Plasma Membrane-associated IκBα

Jeffery S. Russell*† and Philip J. Tofilon†‡

*Department of Experimental Radiation Oncology, The University of Texas M. D. Anderson Cancer Center, Houston, Texas 77030; and †Molecular Radiation Therapeutics Branch, Radiation Oncology Science Program, National Cancer Institute, Bethesda, Maryland 20892

Submitted May 2, 2002; Revised July 3, 2002; Accepted July 10, 2002
Monitoring Editor: Keith R. Yamamoto

In contrast to nuclear factor-κB (NF-κB) activation by tumor necrosis factor-α (TNF-α), the specific processes involved in the activation of this transcription factor by ionizing radiation (IR) have not been completely defined. According to the classical paradigm, a critical event in NF-κB activation is the degradation of IκBα. Data presented herein show that, in contrast to treatment with TNF-α, IR-induced NF-κB activation was not accompanied by degradation of IκBα in the U251 glioblastoma cell line as determined in whole cell lysates. However, treatment with the proteosome inhibitor MG-132 inhibited NF-κB activation induced by IR, suggesting that IκBα degradation was a critical event in this process. To reconcile these results, U251 cell lysates were separated into soluble and insoluble fractions and IκBα levels evaluated. Although IκBα was found in both subcellular fractions, treatment with IR resulted in the degradation of IκBα only in the insoluble fraction. Further subcellular fractionation suggested that the IR-sensitive, insoluble pool of IκBα was associated with the plasma membrane. These data suggest that the subcellular location of IκBα is a critical determinant in IR-induced NF-κB activation.

INTRODUCTION

The transcription factor nuclear factor-κB (NF-κB) is susceptible to activation by a variety of stimuli and conditions (Anderson *et al.*, 1994; Koong *et al.*, 1994; Li and Karin, 1998; Uehara *et al.*, 1999; Gao *et al.*, 2001). Initially, NF-κB was shown to play a major role in the regulation of genes involved in inflammation and immunity (Siebenlist *et al.*, 1994; Pomerantz and Baltimore, 1999) with more recent data indicating that it can also serve as a survival factor protecting cells from undergoing apoptosis in response to stress or toxic insult (Zhang *et al.*, 2000; Bottero *et al.*, 2001a). Given its significance in a number of critical biological processes, there is considerable impetus to define the factors and signaling pathways that regulate NF-κB activation. The biochemical events involved in the activation of NF-κB have been for the most part delineated using cytokines, primarily tumor necrosis factor-α (TNF-α). According to the classical paradigm, NF-κB is sequestered as an inactive complex in the cytoplasm by its inhibitor, IκBα (Siebenlist *et al.*, 1994). Exposure to TNF-α or other stimuli results in the activation of IκB kinase (IKK) (Nasuhara *et al.*, 1999), which phosphorylates IκBα on two specific serine residues (Schottelius *et al.*, 1999). The phosphorylated form of IκBα is then ubiquinated and degraded, unmasking the nuclear localization sequence on NF-κB and allowing it to be imported into the nucleus (Duffey *et al.*, 1999).

Among the agents capable of activating NF-κB is ionizing radiation (IR). However, although there have been a number of reports of IR-induced NF-κB activation in a variety of cell types, there are suggestions that the processes involved differ from those defined for TNF-α. IR induces the activation of NF-κB beginning 2–4 h after exposure with its activity returning to untreated levels by ~8 h (Brach *et al.*, 1991; Mohan and Meltz, 1994; Russell *et al.*, 2002). This is in contrast to TNF-α–mediated activation of NF-κB, which occurs with peak activation at 30 min (Claudio *et al.*, 1996; Raju *et al.*, 1997; Russell *et al.*, 2002). These disparate time courses suggest that there are fundamental differences in the TNF-α– and IR-initiated signaling pathways leading to NF-κB activation. Furthermore, activation of NF-κB by IR was shown to occur in the absence of IκBα degradation in rat astrocytes and the human glioma cell line U373 (Raju *et al.*, 1998). In addition to experimental observations comparing TNF-α and IR, the obvious differences between the agents themselves (i.e., cytokine vs. physical deposition of energy) sug-

Article published online ahead of print. Mol. Biol. Cell 10.1091/mbc.E02–05–0252. Article and publication date are at www.molbiolcell.org/cgi/doi/10.1091/mbc.E02–05–0252.

‡ Corresponding author. E-mail address: tofilonp@mail.nih.gov.

gest the involvement of unique signaling pathways mediating the activation of NF-κB.

In an attempt to define the specific processes involved in IR-induced NF-κB activation, we have evaluated the events previously shown to mediate NF-κB activation after TNF-α treatment. Initial observations indicated that, in contrast to treatment with TNF-α, IR-induced activation of NF-κB in U251 cells was not associated with the degradation of IκBα. However, upon further investigation, the data presented herein show that IκBα degradation is required for IR-induced NF-κB activation and can be detected when the insoluble cell fraction is evaluated. Furthermore, the IκBα located in the plasma membrane seems to be selectively targeted by IR, whereas TNF-α degrades IκBα located in each of the cell fractions examined. Thus, data presented herein suggest that subcellular localization of the IκBα/NF-κB complex can be a determining factor in the susceptibility of NF-κB to IR-induced activation.

MATERIALS AND METHODS

Antibodies and Reagents

Antibodies to nucleoporin, calnexin, BiP, GM130, and VLA-2α were obtained from BD PharMingen (San Diego, CA). Cytochrome *c* oxidase I antibody was from Molecular Probes (Eugene, OR). Antibodies to IκBα, IκBβ, IκBγ, NF-κB p65, epidermal growth factor receptor (EGFR), and hexokinase IV were acquired from Santa Cruz Biotechnology (Santa Cruz, CA). Dimethyl sulfoxide and human TNF-α were purchased from Sigma-Aldrich (St. Louis, MO). Actin antibody was purchased from Chemicon International (Temecula, CA). MG-132 was purchased from BIOMOL Research Laboratories (Plymouth Meeting, PA).

Cell Lines and Culture Conditions

The human glioblastoma cell lines U251 and SF539 and the pancreatic BXPC-3 cell line were obtained from American Type Culture Collection (Manassas, VA) and maintained as described previously (Russell et al., 2002).

Radiation

Cultured monolayer cells were irradiated using a ^{137}Cs source at a dose rate of 3.7 Gy/min (U.S. Nuclear, Burbank, CA).

Electrophoretic Mobility Shift Assay (EMSA)

The preparation of nuclear extracts and EMSA analysis were described previously (Russell *et al.*, 2002).

Separation into Insoluble and Soluble Cell Fractions

Cellular fractionation was performed as described previously (Bergo *et al.*, 2000) with several modifications. Briefly, cell cultures (8×10^6 cells) were washed twice with phosphate-buffered saline (PBS), scraped into 10 ml of PBS, and pelleted at $500 \times g$. The supernatant was aspirated, and the cell pellet was resuspended in three volumes of hypotonic lysis buffer (10 mM Tris, pH 7.4, 0.1 M sucrose, 10 mM NaCl, 1 mM dithiothreitol, 1 mM phenylmethylsulfonyl fluoride, 1 mg/ml aprotinin, 1 mg/ml leupeptin, 250 mg/ml benzamide). The suspension was incubated on ice for 10 min, subjected to three rounds of freezing/thawing, and vortexed for 30 s to ensure complete cell breakage. Samples were spun at $100,000 \times g$ for 60 min at 4°C. The supernatant (S100) was treated with 1% NP-40 and collected as the soluble fraction and stored at −80°C. The pellet (P100) was resuspended in hypotonic lysis buffer with 1% NP-40, incubated on ice for 30 min, and vortexed for 30 s at 10-min intervals. The insoluble fraction was then stored at −80°C. Protein concentrations were determined using the DC protein assay kit (Bio-Rad, Hercules, CA).

Subcellular Fractionation

Subcellular fractionation was performed as described previously (Nantel *et al.*, 1999) with several modifications. Briefly, cell cultures (40×10^6 cells) were washed twice with PBS, scraped into 10 ml of PBS, and pelleted at $500 \times g$. The supernatant was aspirated, and the cell pellet was resuspended in three volumes of hypotonic lysis buffer (see above). The suspension was incubated on ice for 10 min and run three times through a 22-gauge needle to ensure complete cell breakage. Samples were then spun at $500 \times g$ for 5 min at 4°C. The supernatant was removed and held for additional processing. The initial pellet was resuspended in 2 volumes of hypotonic lysis buffer, incubated on ice for 10 min, and spun again at $500 \times g$ for 5 min at 4°C. The washing of the pellet was repeated twice, each time combining the extracted supernatants. Finally, the low-speed pellet (P1) was resuspended in 3 volumes of extraction buffer (20 mM HEPES, pH 7.9, 400 mM NaCl, 1 mM EDTA, 1 mM EGTA, 1% NP-40, 1 mM dithiothreitol, 1 mM phenylmethylsulfonyl fluoride, 1 mg/ml aprotinin, 1 mg/ml leupeptin, 250 mg/ml benzamide) and incubated on ice for 30 min while vortexing for 30 s at 10-min intervals. The combined supernatants were spun at $500 \times g$ for 5 min at 4°C to remove any unbroken cells, remaining nuclei, or other large debris. The supernatant was then transferred to a new Eppendorf tube and spun at $18,000 \times g$ for 30 min at 4°C. The resulting pellet (P2) was resuspended in two volumes of extraction buffer and incubated on ice for 30 min while vortexing for 30 s at 10-min intervals. The remaining supernatant was then spun at $100,000 \times g$ for 60 min at 4°C. The resulting high-speed pellet (P3) was resuspended in one volume of extraction buffer and incubated on ice for 30 min while vortexing for 30 s at 10-min intervals. The supernatant (S100) was collected as the S fraction, treated with 1% NP-40, and incubated on ice for 30 min while vortexing for 30 s at 10-min intervals. Cellular fractions were then stored at −80°C and protein concentrations were subsequently determined using the DC protein assay kit (Bio-Rad).

Sucrose Density Gradients

The P2 pellets were collected as described above and subjected to sucrose density gradient centrifugation as described in Hubbard *et al.* (1983) and Meier *et al.* (1984) with several modifications. Sucrose density gradients were generated by layering three concentrations of sucrose (1.5, 0.75, and 0.375 M; chilled to 4°C) in 3-ml volumes in an ultracentrifuge tube. Samples (P2 pellets) were resuspended in 1 ml of 0.375 M sucrose and added to the top layer. The gradients were then spun at $100,000 \times g$ for 4 h at 4°C. Tubes were then removed and kept on ice. The interface between sucrose layers was collected by inserting an 18-gauge needle into the interface and removing a volume of 1.5 ml. The interface between the 1.5 and 0.75 M sucrose was collected as the lower interface and the interface between the 0.75 and 0.375 M sucrose was collected as the upper interface. The extracted volumes were then resuspended to 3 ml 0.375 sucrose and spun at $100,000 \times g$ for 1 h at 4°C. The supernatant was aspirated and the pellet was resuspended in 1 volume of extraction buffer. Sucrose gradient cell fractions were then stored at −80°C. Protein concentrations were subsequently determined using the DC protein assay kit (Bio-Rad).

Plasma Membrane Isolation

Isolation of a pure plasma membrane fraction is limited by contamination with endoplasmic reticulum (ER) (Hubbard *et al.*, 1983). Lin *et al.* (1988) describe a method of adding $CaCl_2$ to cell lysates to reduce ER contamination and enrich plasma membrane fractions. Direct isolation of the plasma membrane (PM) was performed as

described previously (Lin *et al.*, 1988) with several modifications. Isolation of the P2 pellet was performed as stated above; however, for these studies the pellet was resuspended in 400 μl of hypotonic lysis buffer with $CaCl_2$ added to a final concentration of 10 mM. After incubation on ice for 10 min, the sample was gently vortexed and diluted to 1 ml with 0.375 M sucrose. The $CaCl_2$-treated sample was then subjected to a sucrose density gradient as described above. The lower interface was then isolated, spun down at 100,000 × *g* for 1 h at 4°C, and resuspended in 1 volume of extraction buffer. The PM fraction was then stored at −80°C. Protein concentrations were subsequently determined using the DC protein assay kit (Bio-Rad).

Endoplasmic Reticulum Isolation

Isolation of the ER was achieved as follows. Briefly, cell cultures (40×10^6 cells) were washed twice with PBS, scraped into 10 ml of PBS, and pelleted at 500 × *g*. The supernatant was aspirated and the cell pellet was resuspended in 3 volumes of hypotonic lysis buffer (see above). The suspension was incubated on ice for 10 min and run three times through a 22-gauge needle to ensure complete cell breakage. Samples were then spun at 500 × *g* for 5 min at 4°C. The initial supernatant was removed and discarded. The remaining nuclear pellet was resuspended in 2 volumes of hypotonic lysis buffer and spun at 500 × *g* for 5 min at 4°C. The washing of the pellet was repeated three times. The nuclear washes were then combined and were spun at 500 × *g* for 5 min at 4°C to remove any unbroken cells, remaining nuclei, or other large debris. The supernatant was then diluted to a volume of 1 ml with 0.375 M sucrose. The sample was then subjected to a sucrose density gradient as described above. The lower interface was isolated, spun at 100,000 × *g* for 1 h at 4°C, and resuspended in 1 volume of extraction buffer. The ER fraction was then stored at −80°C. Protein concentrations were subsequently determined using the DC protein assay kit (Bio-Rad).

Immunoblot Analysis

Immunoblot analysis was performed as described previously (Russell *et al.*, 2002).

Confocal Microscopy

Confocal microscopy was performed as described previously (Pepin *et al.*, 1994) with several modifications. Briefly, 1×10^5 cells were plated in four-well chamber slides and allowed to grow for 48 h. Slides were then treated with either radiation (10 Gy) or TNF-α (10 ng/ml). Immediately after treatment the media were replaced with serum-free media containing the EGFR antibody at a 1:50 dilution for 2 h. At the appropriate time point (2 h after IR and 30 min after TNF), the slides were fixed in 4% paraformaldehyde for 2 min and permeabilized for 3 min in a 1% NP-40/PBS solution. Slides were then washed and allowed to incubate with the IκBα antibody at a 1:50 dilution in 1% bovine serum albumin in PBS for 2 h. After washing with PBS, the appropriate secondary antibodies (fluorescein isothiocyanate and Texas Red conjugates) were applied at a dilution of 1:100 in 1% bovine serum albumin for 1 h. Slides were then washed, the chambers removed, and antifade (DAKO, Carpinteria, CA) added to the slide. Coverslips were then applied and sealed with nail polish. Slides were then observed under a laser scanning 510 LSM confocal microscope (Carl Zeiss, Thornwood, NY). Images were captured using LSM software package (Carl Zeiss).

RESULTS

As an initial characterization of radiation-induced NF-κB activation in the human glioma cell line U251, NF-κB/DNA binding was determined as a function of time after exposure to 10 Gy. As shown in Figure 1, there is a relatively low basal level of NF-κB activity in U251 cells, which is increased by IR in a time-dependent manner, reaching a maximum at 2 h and returning to control levels by 8 h after exposure. This time course is in contrast to U251 cells treated with TNF-α, in which case maximal NF-κB activity was induced within 30 min (Russell *et al.*, 2002).

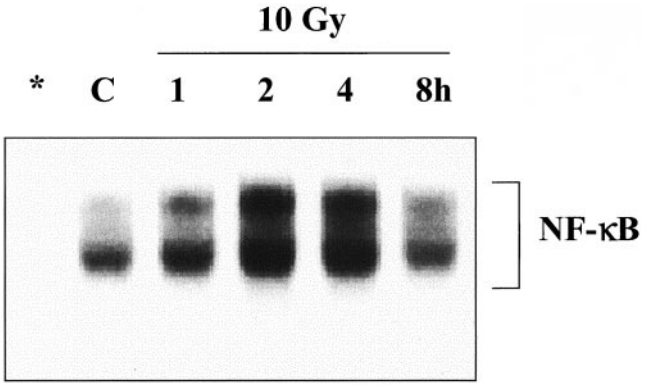

Figure 1. IR-induced NF-κB activation. Cells were irradiated (10 Gy) and collected at the specified times for EMSA analysis. Asterisk (*) indicates lane containing a 100-fold excess of cold NF-κB oligonucleotide competitor. C, unirradiated control sample.

According to the classical paradigm, a critical event in NF-κB activation is the degradation of IκBα, which allows NF-κB to translocate to the nucleus (Karin and Ben Neriah, 2000). Thus, as a further comparison between TNF-α and IR-induced NF-κB activation, IκBα protein levels were determined in U251 whole cell lysates after each treatment. In U251 cells treated with TNF-α, IκBα levels were significantly reduced by 5 min and returned to control levels by 60 min (Figure 2A), consistent with previous reports (Claudio *et al.*, 1996). In contrast, after exposure to IR, no significant degradation of IκBα was detected (Figure 2B). In addition to IκBα, other IκB proteins have been shown to play a role in the regulation of NF-κB activation (Baeuerle and Baltimore, 1996; Renard *et al.*, 2000). To determine whether IκBβ and IκBγ were involved in IR-induced NF-κB in U251 cells, the levels of these two proteins were determined by immunoblot analysis. As shown in Figure 3A, TNF-α exposure resulted in the degradation of IκBβ with the same kinetics as IκBα, but did not affect IκBγ. Treatment with IR had no effect on levels of IκBβ or IκBγ (Figure 3B).

The above-mentioned results suggested that degradation of IκBα is not necessary for radiation-induced NF-κB activation in U251 cells. To test this hypothesis, U251 cells were treated with the proteosome inhibitor MG-132. If IκBα degradation is not required for NF-κB activation in U251 cells, MG-132 should not affect NF-κB DNA binding after IR. However, as shown in Figure 4, MG-132 significantly reduced radiation-induced NF-κB DNA binding activity, indicating that degradation of IκBα is indeed an essential step in IR-induced NF-κB activation.

Because IκBα exists primarily in the cytoplasm, its degradation after exposure to activators of NF-κB is typically evaluated and detected using whole cell lysates, as shown in Figure 2, A and B. However, IκBα has also been detected in other subcellular compartments (Suyang *et al.*, 1996; Hay *et al.*, 1999; Rodriguez *et al.*, 1999; Sachdev *et al.*, 2000). To

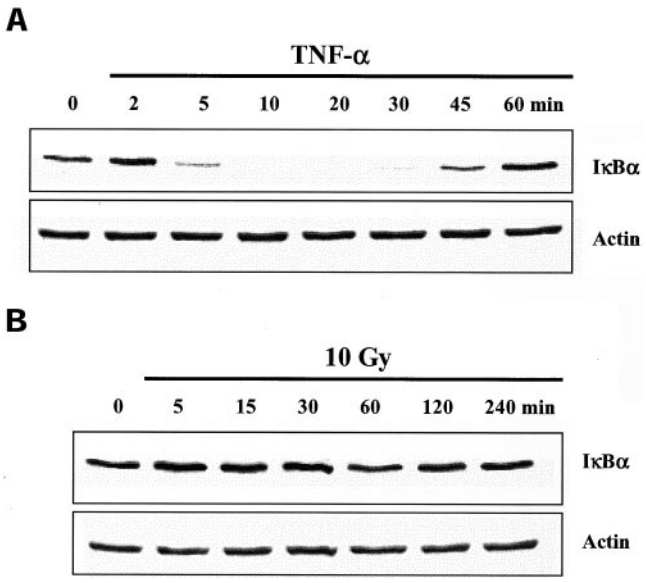

Figure 2. IκBα protein levels in U251 cells after exposure to TNF-α or IR. Cells were treated with TNF-α (10 ng/ml) (A) or irradiated (10 Gy) (B) and collected at the specified times for immunoblot analysis. Actin was used as a loading control. 0, untreated control sample.

determine whether radiation affects IκBα located at other sites, U251 cell lysates were separated into soluble (S) and insoluble (I) fractions (see MATERIALS AND METHODS)

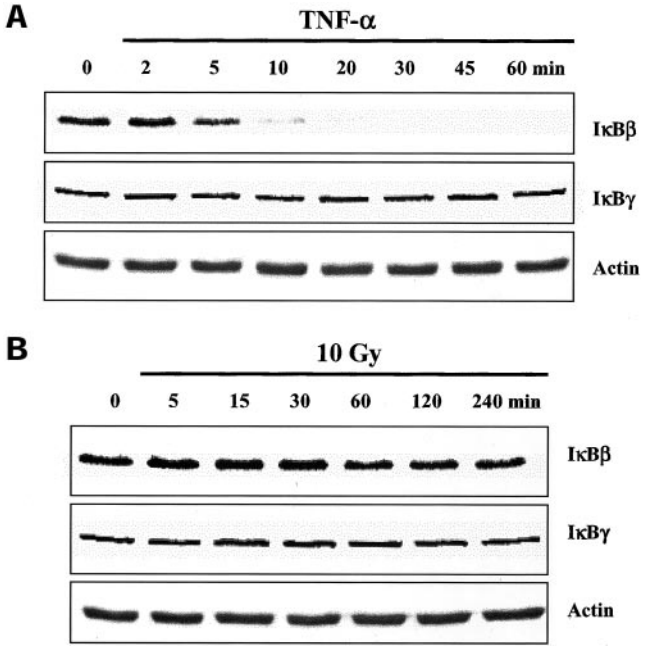

Figure 3. IκBβ and IκBγ protein levels in U251 cells after exposure to TNF-α or IR. Cells were treated with TNF-α (10 ng/ml) (A) or irradiated (10 Gy) (B) and collected at the specified times for immunoblot analysis. Actin was used as a loading control. 0, untreated control sample.

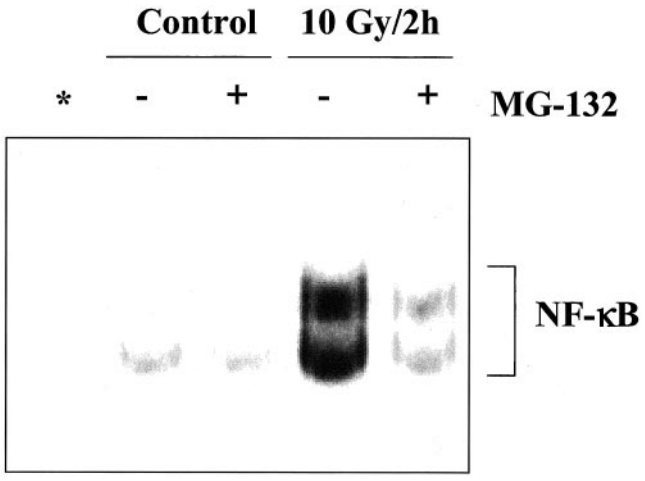

Figure 4. Effect of MG-132 on IR-induced NF-κB activation. Cells were treated with MG132 (50 μM, 2 h) or dimethyl sulfoxide (vehicle control), irradiated (10 Gy), and collected 2 h later for EMSA analysis. Asterisk (*) indicates lane containing a 100-fold excess of cold NF-κB oligonucleotide competitor.

and IκBα levels determined by immunoblot analysis. For these studies, cytochrome *c* oxidase I, which is localized to the mitochondrial membrane, was used as a marker for the insoluble fraction and hexokinase IV, which is found in the cytoplasm, was used as a marker for the soluble fraction (Figure 5). In U251 cells the majority of IκBα is present in the soluble fraction, with a significantly smaller level found in the insoluble fraction. Whereas treatment of U251 cells with TNF-α induced degradation of IκBα in both fractions, exposure of cells to IR had no effect on IκBα levels in the soluble fraction, which corresponds to the cytoplasm, but did result in the loss of IκBα from the insoluble fraction. To examine the effects of IR and TNF-α on the other isoforms of IκB, additional immunoblot analysis was performed on the insoluble and soluble fractions. Although IκBγ was found in both insoluble and soluble fractions, IκBβ was only detected

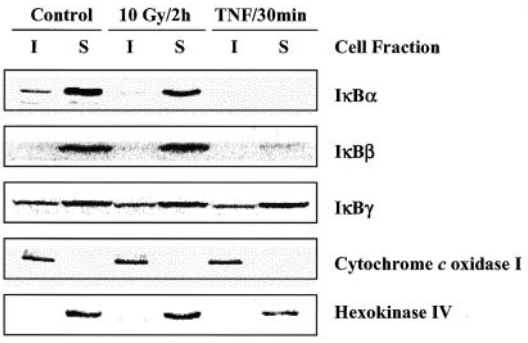

Figure 5. IκBα, IκBβ, and IκBγ protein levels in insoluble and soluble fractions of U251 cells after exposure to IR or TNF-α. Cells were mock irradiated, irradiated (10 Gy, 2 h), or treated with TNF-α (10 ng/ml, 30 min) and collected for immunoblot analysis. Cytochrome *c* oxidase I and hexokinase IV were used as markers of the insoluble and soluble fractions, respectively.

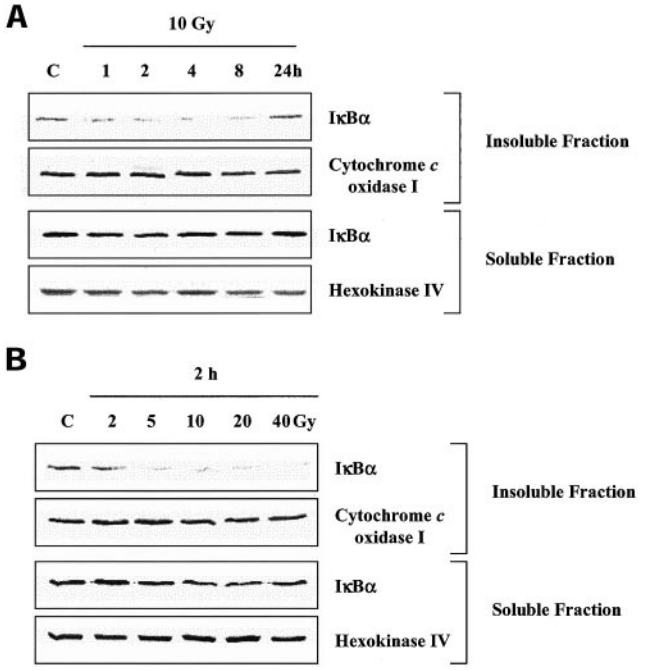

Figure 6. IκBα protein levels in the insoluble and soluble fractions of irradiated U251 cells. (A) Cells were treated with IR (10 Gy), collected at the specified times, separated into insoluble and soluble fractions, and subjected to immunoblot analysis. (B) Cells were treated with the indicated doses of IR, collected after 2 h, separated into insoluble and soluble fractions, and subjected to immunoblot analysis. Cytochrome *c* oxidase I and hexokinase IV were used as markers of the insoluble and soluble fractions, respectively. C, mock-irradiated control sample.

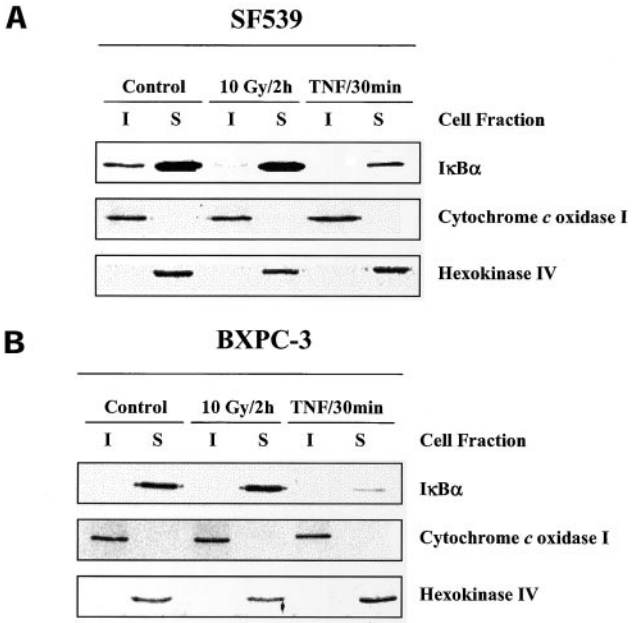

Figure 7. IκBα protein levels in insoluble and soluble fractions of SF539 and BXPC-3 cells after exposure to IR or TNF-α. (A) SF539 cells were mock irradiated, irradiated (10 Gy, 2 h), or treated with TNF-α (10 ng/ml, 30 min), collected, and separated into insoluble and soluble fractions, and subjected to immunoblot analysis. (B) BXPC-3 cells were mock irradiated, irradiated (10 Gy, 2 h), or treated with TNF-α (10 ng/ml, 30 min), collected, separated into insoluble and soluble fractions, and subjected to immunoblot analysis. Cytochrome *c* oxidase I and hexokinase IV were used as markers of the insoluble and soluble compartments, respectively.

in the soluble fraction. Whereas the soluble pool of IκBβ was reduced after TNF-α treatment, IR had no effect on IκBβ or IκBγ levels.

The effects of IR on IκBα located in the insoluble fraction were then characterized as a function of time after irradiation and dose (Figure 6). After 10 Gy a decrease in IκBα levels in the insoluble fraction was detected by 1 h and remained suppressed until 24 h post-IR. No significant change in IκBα levels was detected in the soluble fraction at any of the time points examined after IR. At 2 h after IR, doses as low as 5 Gy resulted in loss of IκBα from the insoluble fraction, whereas doses of up to 40 Gy had no significant effect on IκBα in the soluble fraction. The loss of IκBα from the insoluble fraction is consistent with IR-induced NF-κB activation in terms of dose and time course. Furthermore, these data account for the failure to detect IκBα degradation after IR when whole cell lysates are evaluated. That is, the IκBα located in the soluble fraction (cytoplasm), which is not affected by IR, masks the IR-induced loss of IκBα in the insoluble fraction, which is present in considerably smaller levels.

To determine whether the existence of IR-sensitive IκBα in the insoluble fraction was unique to U251 cells, two additional cell lines were evaluated. Previously, we showed that the SF539 glioma cell line had a low basal level of NF-κB activity, which was significantly increased after 10 Gy IR with the same kinetics as the U251 cell line (Russell *et al.*, 2002). In contrast, the BXPC-3 pancreatic cell line has a relatively high basal level of NF-κB activity that is not enhanced by IR (Russell *et al.*, 2002). Evaluation of immunoblots of whole cell lysates from SF539 and BXPC-3 cell line did not show any degradation of IκBα after 10 Gy IR (our unpublished data). As shown in Figure 7A, when SF539 cell lysates were separated into insoluble and soluble fractions, IκBα is detectable in both fractions; IR induced the loss of IκBα only from the insoluble fraction, whereas treatment with TNF-α resulted in degradation of IκBα located in the insoluble and soluble fractions. These results are similar to those for U251. In contrast, in the BXPC-3 cell line, IκBα was only detected in the soluble fraction, which was reduced after TNF-α treatment but not after IR (Figure 7B). The same markers (cytochrome *c* oxidase I and hexokinase IV) used for U251 cells described above were used as a measure of the effectiveness of the isolation procedure in these cell lines.

As a first step in determining the specific subcellular site(s) in which the IR-sensitive IκBα is located, U251 cell lysates were subjected to serial differential centrifugation (see MATERIALS AND METHODS). Cell lysates were spun at specified rates, which resulted in four fractions (P1, 500 × *g* pellet; P2, 18,000 × *g* pellet; P3, 100,000 × *g* pellet; S, 100,000 × *g* supernatant) and subjected to immunoblot analysis. As shown in Figure 8A, IκBα was found in all three pellets representative of the insoluble fraction (P1, P2, and

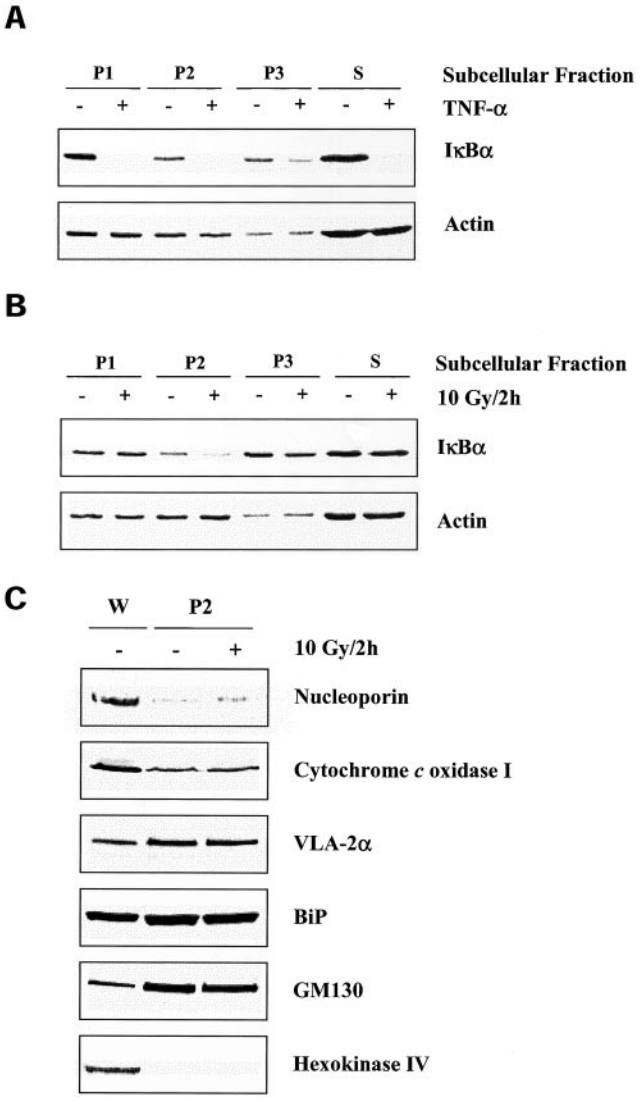

Figure 8. IκBα protein levels in subcellular fractions of U251 cells after exposure to TNF-α or IR. (A) Cells were treated with TNF-α (10 ng/ml, 30 min) or (B) irradiated (10 Gy, 2 h), collected, separated into specified subcellular fractions (see MATERIALS AND METHODS), and subjected to immunoblot analysis. Actin was used as a loading control within a particular subcellular fraction. (C) Identification of organelles localized to P2 fraction of U251 cells. Cells were mock irradiated or irradiated with 10 Gy, collected at 2 h, separated into specified subcellular fractions, and subjected to immunoblot analysis for protein markers of cellular organelles. W, whole cell lysate, which was used as a positive control.

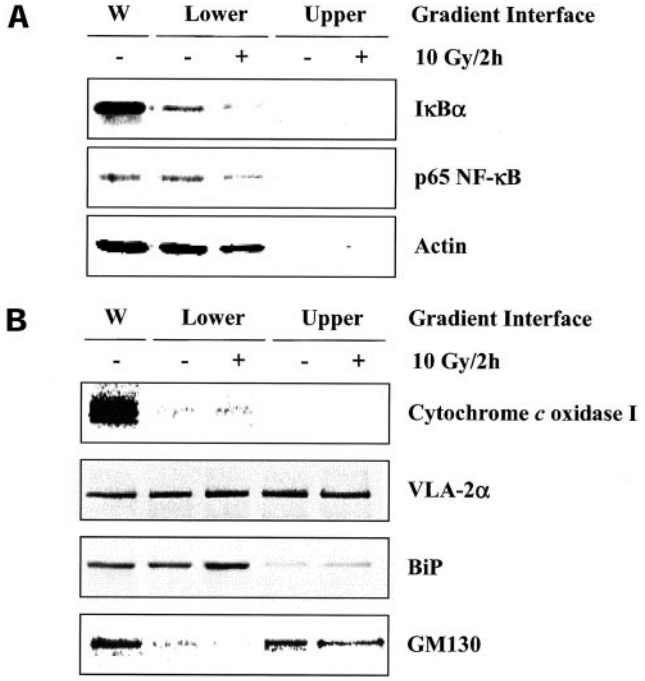

Figure 9. IκBα and p65 NF-κB protein levels after sucrose density gradient separation of the P2 fraction of U251 cells. (A) Cells were mock irradiated or irradiated with 10 Gy, collected at 2 h, separated into specified subcellular fractions, and subjected to a sucrose density gradient (see MATERIALS AND METHODS). Immunoblot analysis was performed on the resulting protein pellet. Actin was used as a loading control within a particular subcellular fraction. (B) Marker proteins corresponding to specific organelles after the P2 fraction was subjected to sucrose density gradient separation. W, whole cell lysate, which served as a positive control.

P3), as well as in the S fraction, which corresponds to the cytoplasm. Whereas TNF-α degraded IκBα in all four fractions (Figure 8A), IR induced the loss of IκBα only from the P2 fraction (Figure 8B). The lack of effect of IR on the pool of IκBα localized to the S fraction as well as the IR-induced degradation of IκBα in an insoluble fraction (P2) was consistent with previous results in this study (Figure 5). To define the organelles found in the P2 fraction, immunoblots were probed with antibodies to specific protein markers corresponding to the nucleus (nucleoporin), mitochondria (cytochrome *c* oxidase I), plasma membrane (VLA-2α), ER (BiP), Golgi (GM130), and cytoplasm (hexokinase IV). As shown in Figure 8C, the P2 pellet, which contained the IR-sensitive IκBα, was composed of mitochondria, plasma membrane, ER, and Golgi complex and was relatively free of nuclei or cytoplasm. None of the organelle markers were affected by treatment with IR.

To delineate the components of the P2 fraction isolated from U251 cells, the P2 pellet was added to a sucrose density gradient (SDG) and subjected to high-speed centrifugation (see MATERIALS AND METHODS). Immunoblot analyses of the SDG interfaces were then performed. As shown in Figure 9A, IκBα and p65 NF-κB were both localized to the lower interface fraction of the SDG. When the same procedure was performed on U251 cells exposed to 10 Gy 2 h previously there was a significant loss of each protein, which is consistent with IκBα being degraded and NF-κB translocating to the nucleus (Karin and Ben Neriah, 2000). To identify the subcellular components in the lower interface of the SDG, the same marker proteins used in Figure 8C were analyzed. As shown in Figure 9B, the lower interface of the SDG, which contained the IR-sensitive IκBα, was enriched in plasma membrane and ER and relatively free of mitochondria or Golgi complexes.

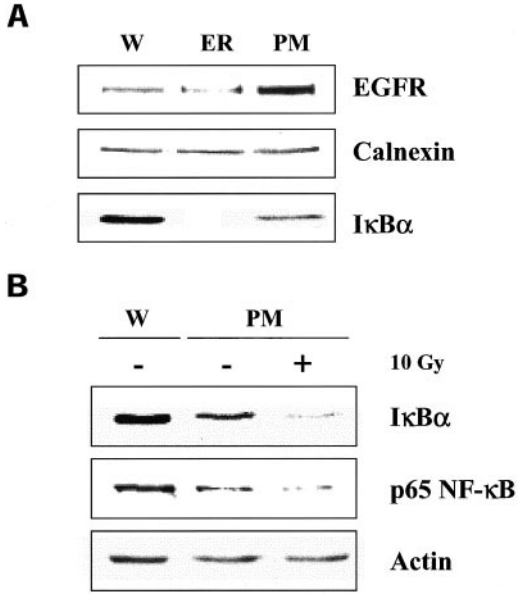

Figure 10. IκBα and p65 NF-κB protein levels in isolated ER and PM fractions of U251 cells. (A) Immunoblot analysis of isolated PM and ER fractions for protein markers (EGFR and calnexin, respectively) and IκBα. (B) Cells were mock irradiated or irradiated with 10 Gy, collected after 2 h, and the PM fraction isolated. Immunoblot analysis was then performed using actin as a loading control. W, whole cell lysate.

The results from Figure 9 suggest that the radiosensitive pool of IκBα is associated with either the ER or PM. To separate ER from the PM it was necessary to use individual isolation schema. For the PM fraction, $CaCl_2$-treated P2 pellets (Lin *et al.*, 1988) were passed through the SDG. The lower interface of the SDG was then isolated and subjected to immunoblot analyses. Enriched ER fractions were obtained from combined washes of the low-speed (nuclear) pellet followed by SDG separation. The lower interface of the SDG was then isolated and subjected to immunoblot analyses. For these studies EGFR and calnexin were used as markers of the PM and ER, respectively. As shown in Figure 10A, enriched ER and PM fractions were obtained as indicated by a decrease of EGFR in the ER fraction and an increase in EGFR in the PM fraction. However, the greatest enrichment was achieved for IκBα, which was only detected in the fraction corresponding to the PM marker. These results suggest that IκBα is preferentially associated with the plasma membrane and not the ER. As shown in Figure 10B, in PM fractions isolated from irradiated U251 cells, there was a significant loss of both IκBα and p65 NF-κB. Thus, these results further suggests that the IR-sensitive pool of IκBα/NF-κB is located in the plasma membrane.

However, because of an inability to more completely reduce the ER component in the PM fraction as shown in Figure 10, confocal microscopy was used as an additional approach to investigate the subcellular location of IR-sensitive IκBα. For this study cells were grown on chamber slides and immunocytochemistry performed using an EGFR antibody to demarcate the PM (green fluorescence) and an antibody to IκBα (red fluorescence). As shown in Figure 11, in control untreated U251 cells IκBα was distributed throughout the cell. Treatment with TNF-α resulted in the complete loss of IκBα, consistent with the immunoblot analysis shown in Figure 2A. In contrast, IR seems to result in the loss of IκBα primarily around the periphery of the cell. Thus, these data along with the cell fractionation studies suggest that IR selectively targets IκBα associated with the plasma membrane.

DISCUSSION

The ability of diverse stimuli such as cytokines, hypoxia, UV radiation, and ionizing radiation to activate NF-κB suggests that this transcription factor is susceptible to activation via a number of signaling pathways (Koong *et al.*, 1994; Li and Karin, 1998; Uehara *et al.*, 1999; Gao *et al.*, 2001). Along these lines, Anderson *et al.* (1994) illustrated the existence of stimuli-specific signaling pathways by showing that oxidative stress (H_2O_2) triggered NF-κB activation in only one of two human T-cell lines, whereas cytokines and phorbol esters stimulated NF-κB in both cell lines. Although the specific processes mediating activation by TNF-α have been well defined, the signaling events involved in NF-κB activation after other stimuli have not been fully elucidated. NF-κB activation by hypoxia involves tyrosine, rather than serine phosphorylation and is accompanied by IκBα degradation (Koong *et al.*, 1994). In contrast, Imbert *et al.* (1996) reported that treatment of Jurkat T cells with pervanadate resulted in tyrosine phosphorylation of IκBα and activation of NF-κB independently of IκBα degradation. Finally, UV-C was shown to activate NF-κB in the absence of an increase in IKK activity (Li and Karin, 1998). Defining the individual signaling pathways that lead to the activation of NF-κB would not only be of fundamental value but may also provide the basis for approaches that inhibit NF-κB activation by a specific agent, yet would not affect NF-κB activation generated by other stimuli.

With respect to IR, it was initially noted that NF-κB activation occurs in the absence of IκBα degradation, that is, based on the analysis of whole cell lysates. The ability of IR to activate NF-κB in the absence of IκBα degradation suggested that IR may, in fact, activate a signaling pathway similar to that of pervanadate involving the tyrosine phosphorylation of IκBα (Imbert *et al.*, 1996). However, we recently showed that exposure of U251 cells to IR resulted in the serine phosphorylation of IκBα (Russell *et al.*, 2002). Furthermore, and more convincingly, data in this report (Figure 4) revealed that proteosome inhibition significantly reduced activation of NF-κB after IR. These results indicated that IκBα degradation was indeed a critical step in IR-induced NF-κB activation, but undetectable using standard approaches.

A possible explanation was that IR was affecting a specific, smaller pool of IκBα. This would be consistent with the relative inefficiency of IR as an activator of NF-κB compared with TNF-α (Li and Karin, 1998; Shao *et al.*, 2001). Whereas the classical paradigm of NF-κB activation defines IκBα as a cytoplasmic protein (Karin and Ben Neriah, 2000), several reports have shown that IκBα can localize or interact with subcellular compartments other than the cytoplasm. IκBα has been detected in the nucleus where it associates with NF-κB dimers and returns them to the cytoplasm as inactive

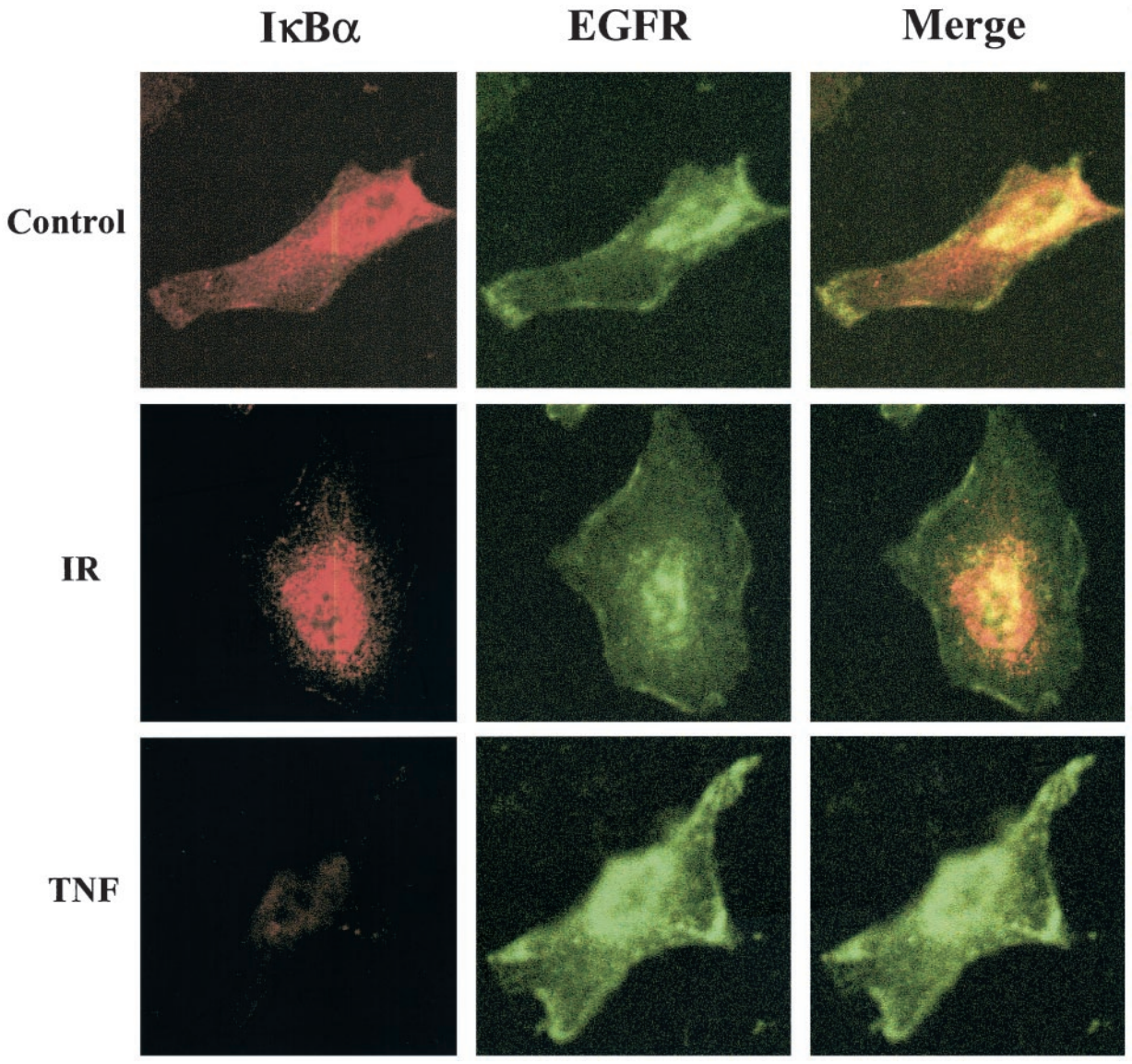

Figure 11. Immunofluorescence localization of IκBα and EGFR (PM marker) in U251 cells after treatment with IR and TNF-α. Cells growing in chamber slides were exposed to IR (10 Gy, 2 h) or TNF-α (10 ng/ml, 30 min) and then incubated with antibodies to EGFR (green fluorescence) and IκBα (red fluorescence). Representative cells are shown as imaged using confocal microscopy.

complexes (Hay *et al.*, 1999; Rodriguez *et al.*, 1999; Sachdev *et al.*, 2000). In addition, Cuervo *et al.* (1998) demonstrated that in Chinese hamster ovary cells IκBα could also be found in lysosomes; under conditions of nutrient deprivation lysosomal IκBα was degraded resulting in the activation of NF-κB. Finally, IκBα can also exist in the mitochondria associated with ANT, a mitochondrial ATP transport protein (Bottero *et al.*, 2001b). To determine whether IR affected a subcellular pool of IκBα other than that located in the cytoplasm, U251 cell lysates were first fractionated into insoluble and soluble components. These initial studies clearly showed that IR resulted in a loss of IκBα in the insoluble cell fraction without having any effect on IκBα in the soluble portion (i.e., the cytoplasmic pool). This is in contrast to treatment with TNF-α, which degraded IκBα in both fractions. However, as shown in Figure 5, the majority of IκBα is localized in the soluble cell fraction consistent with previous studies (Karin and Ben Neriah, 2000), which explains the failure to detect IκBα degradation after IR when using the standard approach of evaluating whole cell lysates. Regarding the other members of the IκB protein family, whereas IκBγ was detected in both the soluble and insoluble fractions, IκBβ was only found in the soluble compartment. Furthermore, IκBβ was degraded after exposure to TNF-α; IκBγ was not affected by treatment with TNF-α or IR. These variations in location and susceptibility to stimuli may reflect the different roles of the IκB family members in the regulation of NF-κB activity (Baeuerle and Baltimore, 1996; Renard *et al.*, 2000).

The localization of IR-sensitive IκBα to the insoluble protein fraction was shown for the U251 and SF539 cells lines, which are both susceptible to IR-induced NF-κB. Interestingly, in the BXPC-3 cell line, which does not activate NF-κB in response to IR, IκBα was only detected in the soluble and not in the insoluble cell fraction. Although these results were generated from only three cell lines, they suggest that IκBα localization plays a role in determining the susceptibility to IR-induced NF-κB activation. However, it should be noted that in HeLa cells, Li and Karin (1998) showed that IR-induced NF-κB activity is accompanied by IκBα degradation in whole cell extracts, although to a smaller extent than detected after TNF-α treatment. This may reflect cell type specificity or different levels of IκBα in the insoluble fraction, such that their loss is not masked by the "dominant" soluble fraction.

Investigations using serial centrifugation narrowed the locale of IR-sensitive IκBα to the ER and/or PM fractions. Further studies attempting to obtain enriched ER and PM fractions combined with confocal microscopy after immunocytochemical analyses suggested that the IR-susceptible IκBα/NF-κB complex is located at the plasma membrane. This was unexpected given that previous work seemed to suggest that IκBα found in the nucleus or mitochondria would be of the most biological significance, i.e., after that found in the cytoplasm (Hay *et al.*, 1999; Rodriguez *et al.*, 1999; Sachdev *et al.*, 2000). However, although clearly detected in these organelles of U251 cells, the IκBα found in the nuclei and mitochondria, like that in the cytoplasm, was not sensitive to IR-induced degradation. The membrane association of IκBα is actually consistent with previous results showing that a single chain antibody fragment targeted to Ras protein inhibits IR-induced NF-κB activation in U251 cells and other cell lines (Russell *et al.*, 2002). This inhibition only occurred in cells that expressed an active form of Ras (Russell *et al.*, 2002). Thus, a possible scenario is that active Ras proteins are involved in recruiting IκBα/NF-κB complexes to the cell membrane. It should be noted that BXPC-3 cells, which do not activate NF-κB after IR and do not have IκBα in the insoluble fraction, also do not contain significant levels of activated Ras (Russell *et al.*, 2002).

The studies presented herein demonstrate that, whereas TNF-α treatment results in degradation of all cellular IκBα, including the dominant pool in the cytoplasm, IR-induced degradation is selective for IκBα located in the insoluble cell component, putatively at the PM. One of the critical questions then raised by this study pertains to the resistance of the cytoplasmic pool of IκBα to IR-induced degradation. A possible explanation may lie in the multiple effects of TNF-α. This cytokine interacts with its specific receptors, which have been mechanistically linked to the signaling pathway regulating IKK and subsequent IκBα phosphorylation and degradation (Pimentel-Muinos and Seed, 1999). However, TNF-α treatment also generates reactive oxygen species (ROS) (Chandel *et al.*, 2001; Kohler *et al.*, 2001) with antioxidant treatment inhibiting TNF-α–induced NF-κB activation (Legrand-Poels *et al.*, 1997). In contrast, IR does not serve as a specific receptor ligand, but it does generate ROS. Thus, the situation may exist in which the soluble (cytoplasmic) pool of IκBα is activated via specific receptor-mediated signaling complexes, but the insoluble pool of IκBα is activated as a result of ROS generation. Thus, whereas IR fails to activate the receptor-mediated signaling pathway necessary for degradation of the soluble pool of IκBα, it does generate ROS sufficient for activation mediated by the insoluble pool of IκBα. In contrast, TNF-α activates both pathways and is considerably more efficient at activating NF-κB. Clearly, additional studies are needed to define the specific signaling pathways mediating IR-induced NF-κB activation. The data presented herein, however, do illustrate that an additional level of regulation of NF-κB activation involves subcellular localization.

ACKNOWLEDGMENTS

We thank Susan Garfield (Confocal Microscopy Core Facility, Laboratory of Experimental Carcinogenesis, National Cancer Institute) for assistance with the confocal microscopy.

REFERENCES

Anderson, M.T., Staal, F.J., Gitler, C., Herzenberg, L.A., and Herzenberg, L.A. (1994). Separation of oxidant-initiated and redox-regulated steps in the NF-κB signal transduction pathway. Proc. Natl. Acad. Sci. USA *91*, 11527–11531.

Baeuerle, P.A., and Baltimore, D. (1996). NF-κB: ten years after. Cell *87*, 13–20.

Bergo, M.O., Leung, G.K., Ambroziak, P., Otto, J.C., Casey, P.J., and Young, S.G. (2000). Targeted inactivation of the isoprenylcysteine carboxyl methyltransferase gene causes mislocalization of K-Ras in mammalian cells. J. Biol. Chem. *275*, 17605–17610.

Bottero, V., Busuttil, V., Loubat, A., Magne, N., Fischel, J.L., Milano, G., and Peyron, J.F. (2001a). Activation of nuclear factor κB through the IKK complex by the topoisomerase poisons SN38 and doxorubicin: a brake to apoptosis in HeLa human carcinoma cells. Cancer Res. *61*, 7785–7791.

Bottero, V., Rossi, F., Samson, M., Mari, M., Hofman, P., and Peyron, J.F. (2001b). IκB-α, the NF-κB inhibitory subunit, interacts with ANT, the mitochondrial ATP/ADP translocator. J. Biol. Chem. *276*, 21317–21324.

Brach, M.A., Hass, R., Sherman, M.L., Gunji, H., Weichselbaum, R., and Kufe, D. (1991). Ionizing radiation induces expression and binding activity of the nuclear factor κB. J. Clin. Invest *88*, 691–695.

Chandel, N.S., Schumacker, P.T., and Arch, R.H. (2001). Reactive oxygen species are downstream products of TRAF-mediated signal transduction. J. Biol. Chem. *276*, 42728–42736.

Claudio, E., Segade, F., Wrobel, K., Ramos, S., Bravo, R., and Lazo, P.S. (1996). Molecular mechanisms of TNFα cytotoxicity: activation of NF-κB and nuclear translocation. Exp. Cell Res. *224*, 63–71.

Cuervo, A.M., Hu, W., Lim, B., and Dice, J.F. (1998). IκB is a substrate for a selective pathway of lysosomal proteolysis. Mol. Biol. Cell *9*, 1995–2010.

Duffey, D.C., Chen, Z., Dong, G., Ondrey, F.G., Wolf, J.S., Brown, K., Siebenlist, U., and Van Waes, C. (1999). Expression of a dominant-negative mutant inhibitor-κBα of nuclear factor-κB in human head and neck squamous cell carcinoma inhibits survival, proinflammatory cytokine expression, and tumor growth in vivo. Cancer Res. *59*, 3468–3474.

Gao, X., Ikuta, K., Tajima, M., and Sairenji, T. (2001). 12-*O*-Tetradecanoylphorbol-13-acetate induces Epstein-Barr virus reactivation via NF-κB and AP-1 as regulated by protein kinase C and mitogen-activated protein kinase. Virology *286*, 91–99.

Hay, R.T., Vuillard, L., Desterro, J.M., and Rodriguez, M.S. (1999). Control of NF-κB transcriptional activation by signal induced proteolysis of IκBα. Phil. Trans. R. Soc. Lond. B Biol. Sci. *354*, 1601–1609.

Hubbard, A.L., Wall, D.A., and Ma, A. (1983). Isolation of rat hepatocyte plasma membranes. I. Presence of the three major domains. J. Cell Biol. *96*, 217–229.

Imbert, V., *et al*. (1996). Tyrosine phosphorylation of IκB-α activates NF-κB without proteolytic degradation of IκB-α. Cell *86*, 787–798.

Karin, M., and Ben Neriah, Y. (2000). Phosphorylation meets ubiquitination: the control of NF-[κ]B activity. Annu. Rev. Immunol. *18*, 621–663.

Kohler, H.B., Huchzermeyer, B., Martin, M., De Bruin, A., Meier, B., and Nolte, I. (2001). TNF-α dependent NF-κB activation in cultured canine keratinocytes is partly mediated by reactive oxygen species. Vet. Dermatol. *12*, 129–137.

Koong, A.C., Chen, E.Y., and Giaccia, A.J. (1994). Hypoxia causes the activation of nuclear factor κB through the phosphorylation of IκBα on tyrosine residues. Cancer Res. *54*, 1425–1430.

Legrand-Poels, S., Zecchinon, L., Piret, B., Schoonbroodt, S., and Piette, J. (1997). Involvement of different transduction pathways in NF-κB activation by several inducers. Free Radical Res. *27*, 301–309.

Li, N., and Karin, M. (1998). Ionizing radiation and short wavelength UV activate NF-κB through two distinct mechanisms. Proc. Natl. Acad. Sci. USA *95*, 13012–13017.

Lin, P.H., Selinfreund, R.H., Wakshull, E., and Wharton, W. (1988). Rapid isolation of plasmalemma from cultured A431 cells: characterization of epidermal growth factor receptors. Anal. Biochem. *168*, 300–305.

Meier, P.J., Sztul, E.S., Reuben, A., and Boyer, J.L. (1984). Structural and functional polarity of canalicular and basolateral plasma membrane vesicles isolated in high yield from rat liver. J. Cell Biol. *98*, 991–1000.

Mohan, N., and Meltz, M.L. (1994). Induction of nuclear factor κB after low-dose ionizing radiation involves a reactive oxygen intermediate signaling pathway. Radiat. Res. *140*, 97–104.

Nantel, A., Huber, M., and Thomas, D.Y. (1999). Localization of endogenous Grb10 to the mitochondria and its interaction with the mitochondrial-associated Raf-1 pool. J. Biol. Chem. *274*, 35719–35724.

Nasuhara, Y., Adcock, I.M., Catley, M., Barnes, P.J., and Newton, R. (1999). Differential IκB kinase activation and IκBα degradation by interleukin-1β and tumor necrosis factor-α in human U937 monocytic cells. Evidence for additional regulatory steps in κB-dependent transcription. J. Biol. Chem. *274*, 19965–19972.

Pepin, N., Roulston, A., Lacoste, J., Lin, R., and Hiscott, J. (1994). Subcellular redistribution of HTLV-1 Tax protein by NF-κB/Rel transcription factors. Virology *204*, 706–716.

Pimentel-Muinos, F.X., and Seed, B. (1999). Regulated commitment of TNF receptor signaling: a molecular switch for death or activation. Immunity *11*, 783–793.

Pomerantz, J.L., and Baltimore, D. (1999). NF-κB activation by a signaling complex containing TRAF2, TANK and TBK1, a novel IKK-related kinase. EMBO J. *18*, 6694–6704.

Raju, U., Gumin, G.J., Noel, F., and Tofilon, P.J. (1998). IκBα degradation is not a requirement for the X-ray-induced activation of nuclear factor κB in normal rat astrocytes and human brain tumor cells. Int. J. Radiat. Biol. *74*, 617–624.

Raju, U., Lu, R., Noel, F., Gumin, G.J., and Tofilon, P.J. (1997). Failure of a second X-ray dose to activate nuclear factor κB in normal rat astrocytes. J. Biol. Chem. *272*, 24624–24630.

Renard, P., Percherancier, Y., Kroll, M., Thomas, D., Virelizier, J.L., Arenzana-Seisdedos, F., and Bachelerie, F. (2000). Inducible NF-κB activation is permitted by simultaneous degradation of nuclear IκBα. J. Biol. Chem. *275*, 15193–15199.

Rodriguez, M.S., Thompson, J., Hay, R.T., and Dargemont, C. (1999). Nuclear retention of IκBα protects it from signal-induced degradation and inhibits nuclear factor κB transcriptional activation. J. Biol. Chem. *274*, 9108–9115.

Russell, J. S., Raju, U., Gumin, G. J., Lang, F. F., Wilson, D. R., Huet, T., Tofilon, P. J. (2002). Inhibition of radiation-induced nuclear factor-κB activation by an anti-Ras single-chain antibody fragment: lack of involvement in radiosensitization. Cancer Res. *62*, 2318–2326.

Sachdev, S., Bagchi, S., Zhang, D.D., Mings, A.C., and Hannink, M. (2000). Nuclear import of IκBα is accomplished by a ran-independent transport pathway. Mol. Cell Biol. *20*, 1571–1582.

Schottelius, A.J., Mayo, M.W., Sartor, R.B., and Baldwin, A.S., Jr. (1999). Interleukin-10 signaling blocks inhibitor of κB kinase activity and nuclear factor κB DNA binding. J. Biol. Chem. *274*, 31868–31874.

Shao, R., Tsai, E.M., Wei, K., von Lindern, R., Chen, Y.H., Makino, K., and Hung, M.C. (2001). E1A inhibition of radiation-induced NF-κB activity through suppression of IKK activity and IκB degradation, independent of Akt activation. Cancer Res. *61*, 7413–7416.

Siebenlist, U., Franzoso, G., and Brown, K. (1994). Structure, regulation and function of NF-κB. Annu. Rev. Cell Biol. *10*, 405–455.

Suyang, H., Phillips, R., Douglas, I., and Ghosh, S. (1996). Role of unphosphorylated, newly synthesized IκBβ in persistent activation of NF-κB. Mol. Cell Biol. *16*, 5444–5449.

Uehara, T., Matsuno, J., Kaneko, M., Nishiya, T., Fujimuro, M., Yokosawa, H., Nomura, Y. (1999). Transient nuclear factor κB (NF-κB) activation stimulated by interleukin-1β may be partly dependent on proteasome activity, but not phosphorylation and ubiquitination of the IκBα molecule, in C6 glioma cells. Regulation of NF-κB linked to chemokine production. J. Biol. Chem. *274*, 15875–15882.

Zhang, S.Q., Kovalenko, A., Cantarella, G., and Wallach, D. (2000). Recruitment of the IKK signalosome to the p55 TNF receptor: RIP and A20 bind to NEMO (IKKγ) upon receptor stimulation. Immunity *12*, 301–311.